Pressure Enhancement of the Giant Magnetocaloric Effect in $Tb_5Si_2Ge_2$

L. Morellon,[1,*] Z. Arnold,[2] C. Magen,[1] C. Ritter,[3] O. Prokhnenko,[2] Y. Skorokhod,[2] P. A. Algarabel,[1] M. R. Ibarra,[1] and J. Kamarad[2]

[1]*Departamento de Física de la Materia Condensada and Instituto de Ciencia de Materiales de Aragón, Universidad de Zaragoza and Consejo Superior de Investigaciones Científicas, 50009 Zaragoza, Spain*
[2] *Institute of Physics AS CR, Na Slovance 2, 182 21 Prague 8, Czech Republic*
[3]*Institut Laue-Langevin, Boîte Postale 156, 38042 Grenoble Cédex 9, France*

(Received 20 May 2004; published 20 September 2004; publisher error corrected 28 September 2004)

Effects of temperature and pressure on magnetic, elastic, structural, and thermal properties of $Tb_5Si_2Ge_2$ have been studied by means of macroscopic (thermal expansion and magnetization) and microscopic (neutron powder diffraction) techniques. We present evidence that the high-temperature second-order ferromagnetic transition can be coupled with the low-temperature first-order structural phase change into a single first-order magnetic-crystallographic transformation at and above a tricritical point in the vicinity of 8.6 kbar. This pressure-induced coupling has a remarkable effect on the magnetocaloric effect, transforming $Tb_5Si_2Ge_2$ from an ordinary into a giant magnetocaloric effect material.

DOI: 10.1103/PhysRevLett.93.137201 PACS numbers: 75.30.Sg, 62.50.+p, 75.25.+z, 75.30.Kz

Magnetic refrigeration is an emerging technology with a potential to soon become an alternative to the existing vapor-compression approach [1–3]. Magnetic cooling is based on the magnetocaloric effect (MCE), an intrinsic thermodynamic property of magnetic solids, which manifests as an adiabatic temperature change or as an isothermal magnetic entropy change. Worldwide quest for materials exhibiting large MCE's near room-temperature in order to improve existing prototypes is currently underway. Some of the latest examples include $MnFeP_{1-x}As_x$ [4], $MnAs_{1-x}Sb_x$ [5] and $La(Fe_xSi_{1-x})_{13}$ [6], many others can be found in recent reviews [7–9].

The $R_5(Si_xGe_{1-x})_4$ system, where R = rare earth element, is a unique family of giant MCE materials [10] where a remarkable physics has been found [11] including strong magnetoelastic effects [12], and giant magnetoresistance [13]. The observed phenomenology has been associated with an intrinsically layered crystallographic structure built by stacking two-dimensional sub-nanometer-thick layers (slabs) interconnected via partially covalent interslab (Si,Ge)–(Si,Ge) bonds [14]. Three different crystal structures are observed at room-temperature depending on the Si/Ge ratio for the R = Gd series [15], which are intimately related to the number of formed interslab covalentlike bonds: the O(I) orthorhombic (*Pnma*) structure where all bonds are formed; the O(II) orthorhombic structure (*Pnma*) with no interslab bonds; and the monoclinic (M) $P112_1/a$ structure where every other bond is broken. The formation or cleavage of these bonds by changing external parameters such as temperature, magnetic field, or hydrostatic pressure [10–21] results in dramatic crystallographic, electronic, and magnetic changes, thus explaining the powerful magnetoresponsive properties of these materials.

$Tb_5(Si_xGe_{1-x})_4$ is the second best studied series [22–27] where a comprehensive neutron diffraction characterization has been possible [26,27] due to the absence of Gd, an element with an enormous neutron absorption cross section. Alloys with intermediate compositions $0.4 \leq x \leq 0.6$ present a paramagnetic (PM) M structure at room-temperature, the ground state being ferromagnetic (FM) and O(I). Unlike the $Gd_5(Si_xGe_{1-x})_4$ alloys where a coupled first-order M(PM) $\rightarrow$ O(I)(FM) transition takes place on cooling, long-range ferromagnetism sets in $Tb_5Si_2Ge_2$ within the monoclinic phase at T_C before the M $\rightarrow$ O(I) structural transformation takes place at T_t [27]. As a result, the structural and magnetic transitions are no longer coupled in this system, and on cooling the following phase sequence is observed: M(PM) $\rightarrow$ M(FM) $\rightarrow$ O(I)(FM). A decoupling of the magnetic and structural transformations has also been observed in Er_5Si_4 [28].

Recently, we reported that under hydrostatic pressure the transition temperature at the second-order boundary is rather moderately affected ($+0.3$–0.7 K/kbar), whereas pressure effect is significantly stronger ($+3$ K/kbar) at the first-order magneto-structural line when R = Gd [21]. The effect of pressure is, therefore, that of enhancing the interlayer interactions, favoring the ferromagnetic O(I) state as also demonstrated for Gd_5Ge_4 [20]. Within this approach, application of hydrostatic pressure in $Tb_5Si_2Ge_2$ should lead to a moderate increase of the second-order Curie temperature T_C, a much stronger effect is expected at the first-order structural transformation T_t. In this Letter, we report a comprehensive study of the temperature-pressure (T–P) phase diagram of $Tb_5Si_2Ge_2$ by means of thermal expansion, magnetization, and neutron powder diffraction experiments under hydrostatic pressure. A coupling of the fer-

romagnetic transition with the structural change ($T_C = T_t$) is demonstrated at a tricritical point in the vicinity of 8.6 kbar. The impact of coupling magnetic and crystal lattices on the MCE of this material is evaluated allowing to quantify the relative contributions of the change in the crystallographic and magnetic structures to the total entropy in a single alloy.

Details on the preparation and characterization of $Tb_5Si_2Ge_2$ can be found in Refs. [22] and [26]. Linear thermal expansion (LTE) measurements under pressure up to 11 kbar (room-temperature value) were performed using the strain-gauge technique in a standard CuBe piston-cylinder cell. A mixture of mineral oils was used as the pressure transmitting medium and the pressure values at different temperatures were determined using a Manganin pressure sensor. A miniature hydrostatic pressure cell was used for magnetization measurements in a commercial (Quantum Design Ltd.) SQUID magnetometer. The pressure value was determined at low temperatures using the known pressure dependence of the critical temperature of the superconducting state of a Pb sensor placed inside the cell. The magnetization has been measured under pressures up to 9.7 kbar (value at 7 K) at temperatures from 5 to 300 K and in magnetic fields up to 50 kOe.

Neutron diffraction experiments were carried out on the high-intensity two-axis diffractometer D20 ($\lambda = 2.40$ Å) at the ILL, Grenoble. Neutron diffraction patterns were dynamically acquired at temperatures ranging from 75 to 125 K (cooling runs), at atmospheric pressure and under a hydrostatic pressure of 9 kbar by means of a standard stainless steel clamped cell.

In Fig. 1(a) we display the LTE of $Tb_5Si_2Ge_2$ (block symbols) at different values of the applied hydrostatic pressure. A large jump, observed in the LTE, is associated with the first-order M(FM) $\leftrightarrow$ O(I)(FM) crystallographic transition [26,27] at $T_t \cong 93$ K (heating). This change in the structure takes place within the ferromagnetic phase since long-range ferromagnetism is destroyed at higher temperatures within the M structure [27]. This is clearly seen in the zero-pressure low-field (500 Oe) magnetization measurements (open symbols) where $T_C \cong 111$ K. The structural transition is also seen in magnetization measurements as a small steplike anomaly at T_t, e.g., as indicated by a vertical arrow under 0 kbar in the figure and as can be seen in more detail in the inset. Combination of LTE and magnetization measurements has allowed determining the evolution of both structural and magnetic changes upon application of hydrostatic pressure. The obtained T–P phase diagram is shown in Fig. 1(b) where the transition temperature values have been taken at the maximum derivative of the corresponding macroscopic property being monitored (for the sake of clarity, only values upon heating the sample are displayed). It is worth noting the good agreement between

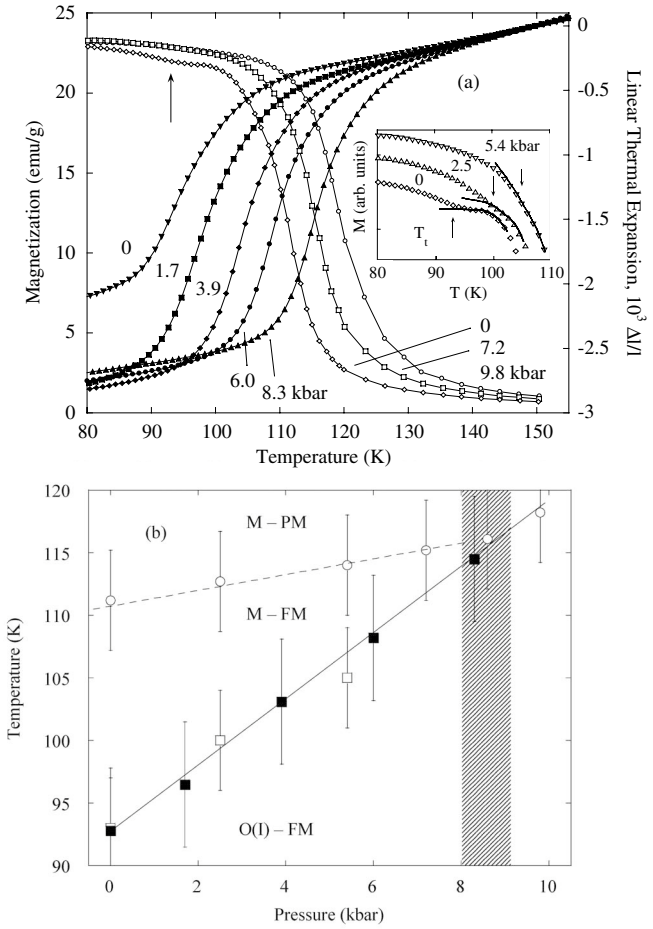

FIG. 1. (a) Magnetization (open symbols) and LTE (block symbols) under selected values of hydrostatic pressure of $Tb_5Si_2Ge_2$ measured on heating. The inset shows a detail of the magnetization vs. temperature curves in the vicinity of T_t. The pressure values have been determined at the transition temperatures. (b) Temperature-pressure phase diagram as determined from magnetization (open circles and squares) and LTE (block squares) data. The dashed and solid lines depict the second-order and first-order transition lines, respectively. The hatched area signals the vicinity of the tricritical point.

the T_t values as determined from the LTE and magnetization data. Consistent with the $Gd_5(Si_xGe_{1-x})_4$ series [20,21], both T_t and T_C shift linearly with pressure to higher temperatures at rates $dT_t/dP = +2.64(6)$ K/kbar and, at $P < 8$ kbar, $dT_C/dP = +0.54(3)$ K/kbar, see Fig. 1(b). For the dT_C/dP only the values below 8 kbar have been determined since both first-order (solid line) and second-order (dashed line) phase boundaries merge at a tricritical point at ~8.6 kbar. Above this pressure, a coupled magnetic-crystallographic transformation M(PM) $\leftrightarrow$ O(I)(FM) takes place.

In order to confirm macroscopic measurements, we carried out neutron powder diffraction experiments under a hydrostatic pressure of 9 kbar. A zero-pressure thermal scan was also required in order to account for the effect of

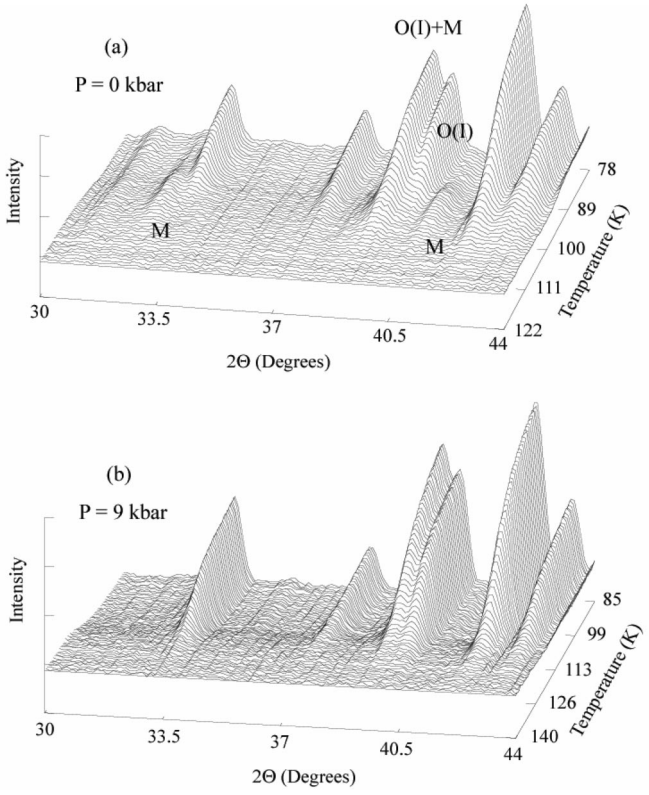

FIG. 2. Thermodiffractogram of $Tb_5Si_2Ge_2$ in zero-pressure (a) and under a 9 kbar hydrostatic pressure (b) in a selected angular range as measured in the high-intensity two-axis diffractometer D20 on cooling. The O(I), M, and O(I) + M diffraction peaks are purely magnetic in origin.

the pressure cell. In Fig. 2, strong differences in the three-dimensional thermodiffractogram in a selected angular range are clearly visible. The marked diffraction peaks are purely magnetic in origin coming from the M, O(I) or both [O(I) + M] phases. The M(FM) peaks at zero-pressure are consistent with a previous study [27], yet they are no longer present at 9 kbar [Fig. 2(b)]. In Fig. 3, the integrated intensities of these three magnetic reflections as functions of temperature under 9 kbar are shown. The results at 0 kbar have been included in the inset. Thus, magnetic scattering demonstrates the existence of a coupled first-order M(PM) $\leftrightarrow$ O(I)(FM) transformation under 9 kbar below $\cong$ 120 K as expected from the T–P phase diagram obtained from macroscopic measurements [Fig. 1(b)]. It is also interesting to note that we have detected magnetic intensity [not clearly seen in Fig. 2(b)] of the M phase below $\cong$ 114 K. This reflects the ferromagnetic ordering of the remaining fraction of M(PM) phase in the two-phase region where O(I)(FM) and M(PM) coexist, in reasonable agreement with the shift of T_C with pressure as determined previously. Therefore, including the regions where different phases coexist, the sequence of structural and magnetic transitions on cooling are as follows: M(PM) $\rightarrow$ M(FM) $\rightarrow$ [M(FM) + O(I)(FM)] $\rightarrow$ O(I)(FM) at $P = 0$, and M(PM) $\rightarrow$ [M(PM) + O(I)(FM)] $\rightarrow$ [M(FM) + O(I)(FM)] $\rightarrow$ O(I)(FM) at $P = 9$ kbar.

The magnetic entropy change ΔS_M has been calculated as described in Ref. [1] using magnetization isotherms measured in the 70-150 K temperature interval every 2.5 K in magnetic fields up to 50 kOe under several values of the hydrostatic pressure. To our knowledge, this is the first time the impact of an applied hydrostatic pressure on the magnetocaloric effect of a material has been reported. We display the results in Fig. 4 for a magnetic field change of $\Delta H = 50$ kOe. In a recent Letter, Pecharsky et al. [17] suggested that in systems with first-order magneto-structural transitions, such as $R_5(Si_xGe_{1-x})_4$, the giant MCE is the sum of the conventional magnetic entropy-driven process, plus the difference in entropy of the two crystallographic modifications, ΔS_{st}:

$$(\Delta S)_T = (\Delta S_M)_T + (\Delta S_{st})_T = \mu_0 \int_0^H \left(\frac{\partial M}{\partial T}\right)_H dH + (\Delta S_{st})_T \qquad (1)$$

Although ΔS_{st} is a hidden parameter in conventional magnetization measurements, ΔS_{st} has been estimated to account for more than a half of the total MCE in low magnetic fields by comparing with other members of the 5:4 family without first-order magneto-structural transformations [17]. To date, a quantitative determination of both contributions in a single alloy has not been achieved and, therefore, $Tb_5Si_2Ge_2$ represents a unique scenario to

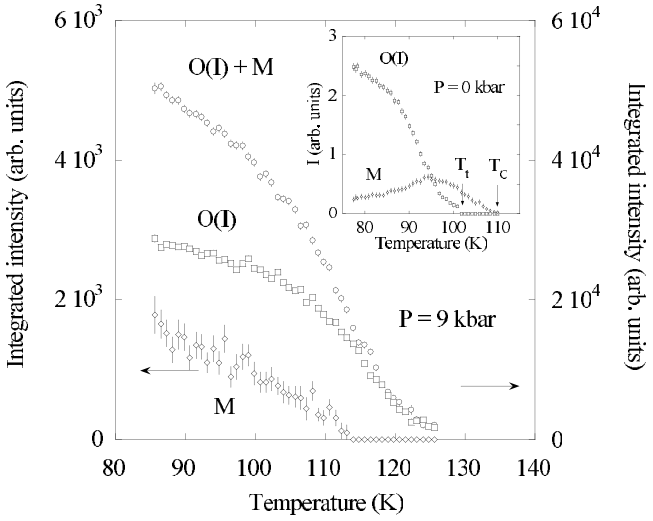

FIG. 3. Temperature dependence of the integrated intensity of selected (marked in Fig. 2, the M peak used being the one at higher angles) purely magnetic diffraction peaks as determined from D20 data under 9 kbar. This experiment was performed on cooling the sample. For comparison, the inset displays the thermal dependence of the O(I) and M magnetic peaks in zero pressure.

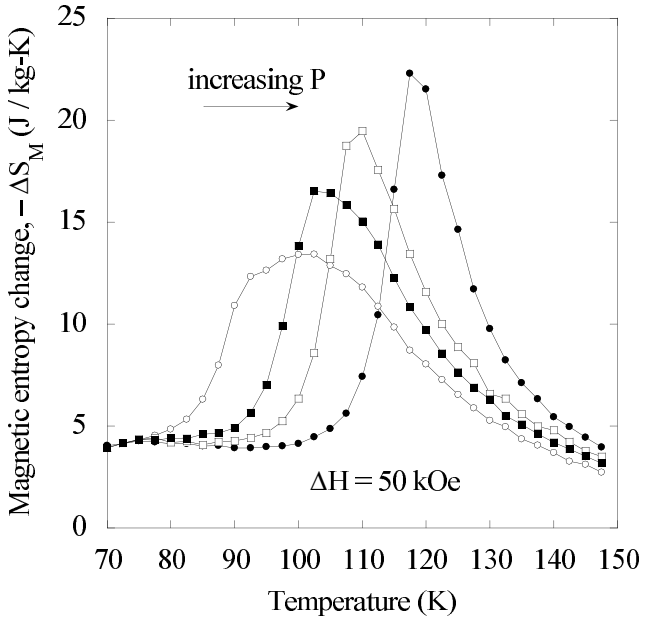

FIG. 4. Magnetocaloric effect in $Tb_5Si_2Ge_2$ for a 50 kOe magnetic field change under the following hydrostatic pressures: 0 (○), 3.4 (■), 6 (□), and 10.2 (●) kbar (pressure values are at the maximum of the entropy change).

analyze Eq. (1), since we can change from a second-order to a first-order transformation by applying hydrostatic pressure to the sample. That is indeed what is observed in Fig. 4. In zero pressure, the maximum of the entropy change amounts to $|\Delta S|$ (T_C, $P = 0$ kbar) = 13.4 J/kg-K, this being an upper limit for $|\Delta S_M|$. Once the two transitions in $Tb_5Si_2Ge_2$ merge at high pressures, a significantly higher value of 22.1 J/kg-K is obtained, and therefore we can obtain $|\Delta S_{st}|$ by using Eq. (1) as $|\Delta S_{st}| = |\Delta S|(9\text{ kbar}) - |\Delta S|(0\text{ kbar}) > 9$ J/kg-K. This value is in reasonable agreement, considering the differences in the transition temperature values, with the 9.3 J/kg-K estimated for the $Gd_5(Si_xGe_{1-x})_4$ series [17], thus supporting all of the above discussion.

As is also observed in Fig. 4, the application of pressure changes significantly the shape of the entropy change of the sample, the peak being sharper as we approach the tricritical point. Nevertheless, by integrating the MCE curves in Fig. 4 over the whole temperature range, we obtained a constant value for the areas of 596(8) J/kg, this being consistent with the sum rule [9] (we have confirmed the saturation magnetization to be virtually independent of pressure by measuring magnetization isotherms at 5 K under pressure, not shown here).

In conclusion, we have determined the temperature-pressure phase diagram of $Tb_5Si_2Ge_2$ by means of thermal expansion, magnetization, and neutron powder diffraction under hydrostatic pressure, a tricritical point being found in the vicinity of 8.6 kbar. The tricritical point signals collapse of the high-temperature second-order magnetic transition with the low-temperature first-order crystallographic transformation. Merging two transformations has a tremendous impact on the shape and maximum value of the magnetocaloric effect, the value of the purely crystallographic contribution to the total entropy change has been quantified to be over 9 J/kg-K, or nearly 40% of the MCE for $\Delta H = 50$ kOe.

The financial support of Project No. 106/02/0943 GA CR is acknowledged.

*Electronic address: morellon@unizar.es

[1] V. K. Pecharsky and K. A. Gschneidner, Jr., J. Magn. Magn. Mater. **200**, 44 (1999).
[2] C. B. Zimm *et al.*, Adv. Cryog. Eng. **43**, 1759 (1998).
[3] C. B. Zimm *et al.*, U.S. Patent No. 6 526 759 (2003).
[4] O. Tegus *et al.*, Nature (London) **415**, 150 (2002).
[5] H. Wada and Y. Tanabe, Appl. Phys. Lett. **79**, 3302 (2001).
[6] A. Fujita *et al.*, Phys. Rev. B **67**, 104416 (2003).
[7] O. Tegus *et al.*, Physica B (Amsterdam) **319**, 174 (2002).
[8] K. A. Gschneidner, Jr. and V. K. Pecharsky, Annu. Rev. Mater. Sci. **30**, 387 (2000).
[9] A. M. Tishin, in *Handbook of Magnetic Materials*, edited by K. H. J. Buschow (Elsevier, New York, 1999), Vol. 12, pp. 395–524.
[10] V. K. Pecharsky and K. A. Gschneidner, Jr., Phys. Rev. Lett. **78**, 4494 (1997); Appl. Phys. Lett. **70**, 3299 (1997); J. Magn. Magn. Mater. **167**, L179 (1997).
[11] V. K. Pecharsky and K. A. Gschneidner, Jr., Adv. Mater. **13**, 683 (2001).
[12] L. Morellon *et al.*, Phys. Rev. B **58**, 14721(R) (1998); **62**, 1022 (2000).
[13] L. Morellon *et al.*, Appl. Phys. Lett. **73**, 3462 (1998); J. Magn. Magn. Mater. **237**, 119 (2001); E. M. Levin, V. K. Pecharsky, and K. A. Gschneidner, Jr., Phys. Rev. B **60**, 7993 (1999).
[14] W. Choe *et al.*, Phys. Rev. Lett. **84**, 4617 (2000).
[15] V. K. Pecharsky and K. A. Gschneidner, Jr., J. Alloys Compd. **260**, 98 (1997); A. O. Pecharsky *et al.*, J. Alloys Compd. **338**, 126 (2002).
[16] C. Magen *et al.*, J. Phys. Condens. Matter **15**, 2389 (2003).
[17] V. K. Pecharsky *et al.*, Phys. Rev. Lett. **91**, 197204 (2003); A. P. Holm *et al.*, Rev. Sci. Instrum. **75**, 1081 (2004).
[18] V. K. Pecharsky *et al.*, J. Solid State Chem. **171**, 57 (2003).
[19] D. H. Ryan *et al.*, Phys. Rev. Lett. **90**, 117202 (2003).
[20] C. Magen *et al.*, Phys. Rev. Lett. **91**, 207202 (2003).
[21] L. Morellon *et al.*, J. Phys. Condens. Matter **16**, 1623 (2004).
[22] L. Morellon *et al.*, Appl. Phys. Lett. **79**, 1318 (2001).
[23] H. Huang *et al.*, Adv. Cryog. Eng. **48**, 11 (2002).
[24] N. P. Thuy *et al.*, J. Magn. Magn. Mater. **242–245**, 841 (2002).
[25] O. Tegus *et al.*, J. Appl. Phys. **91**, 8534 (2002).
[26] C. Ritter *et al.*, Phys. Rev. B **65**, 094405 (2002).
[27] L. Morellon *et al.*, Phys. Rev. B **68**, 024417 (2003).
[28] V. K .Pecharsky *et al.*, Phys. Rev. Lett. **91**, 207205 (2003).